Proceedings of the 3rd World Congress on
Automation & Robotics 2017
28-29 June. San Diego, USA

Advanced Issues of Wind Turbine Modelling and Control[1]

Silvio Simani[2]

Department of Engineering, University of Ferrara. Via Saragat 1E – 44123 Ferrara (FE), Italy

E-mail: silvio.simani@unife.it

Abstract. The motivation for this paper comes from a real need to have an overview about the challenges of modelling and control for very demanding systems, such as wind turbine systems, which require reliability, availability, maintainability, and safety over power conversion efficiency. These issues have begun to stimulate research and development in the wide control community particularly for these installations that need a high degree of "sustainability". Note that this topic represents a key point mainly for offshore wind turbines with very large rotors, since they are characterised by challenging modelling and control problems, as well as expensive and safety critical maintenance works. In this case, a clear conflict exists between ensuring a high degree of availability and reducing maintenance times, which affect the final energy cost. On the other hand, wind turbines have highly nonlinear dynamics, with a stochastic and uncontrollable driving force as input in the form of wind speed, thus representing an interesting challenge also from the modelling point of view. Suitable control methods can provide a sustainable optimisation of the energy conversion efficiency over wider than normally expected working conditions. Moreover, a proper mathematical description of the wind turbine system should be able to capture the complete behaviour of the process under monitoring, thus providing an important impact on the control design itself. In this way, the control scheme could guarantee prescribed performance, whilst also giving a degree of "tolerance" to possible deviation of characteristic properties or system parameters from standard conditions, if properly included in the wind turbine model itself. The most important developments in advanced controllers for wind turbines are addressed, and open problems in the areas of modelling of wind turbines are also outlined.

1. Introduction

Wind energy represents a fast–developing interdisciplinary field comprising many different branches of engineering and science. According to the National Renewable Energy Laboratory (NREL), from 2002 to 2007 the installed capacity of wind grew at a rate of about 30% from 2002 to 2007 [1]. This situation is depicted in Fig. 1.

It can be seen how global wind power installations increased by $35,467$ in 2013, bringing total installed capacity up to 318,137 MW. During 2010–2011 more than half of all new wind power was added outside of the traditional markets of Europe and North America, mainly driven by the continuing boom in China which accounted for nearly half of all of the installations at 18,000 MW in 2011. China now has 91,424 MW of wind power installed. Several countries have

[1] Invited plenary paper.
[2] Invited plenary speaker.

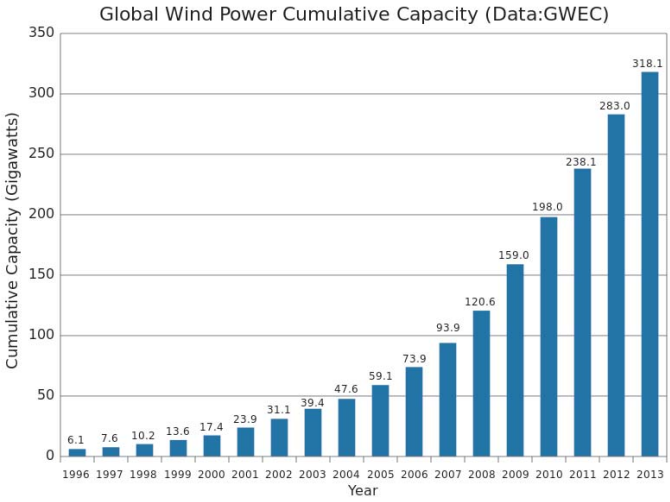

Figure 1. The installed wind energy capacity [2].

achieved relatively high levels of wind power penetration, such as 21% of stationary electricity production in Denmark, 18% in Portugal, 16% in Spain, 14% in Ireland, and 9% in Germany in 2010 [3, 4]. As of 2011, 83 countries around the world are using wind power on a commercial basis. It is clear why wind power is recognised as an effective and green solution for energy harvesting. However, even if the U.S. receives less than 2% of its electrical energy from wind, NREL report lays the framework for achieving 20% of the U.S. electrical energy generation from wind in U.S. by the year 2030 [3, 4]. Despite the expected growth in the installed capacity of wind turbines in recent years, engineering and science challenges still exist. Since wind turbine installations must guarantee both power capture and economical advantages, also the size of wind turbines has grown dramatically from 1980 [3, 4].

Modern wind turbines have large, flexible structures operating in uncertain environments, thus representing interesting cases for advanced control solutions [5]. Advanced controllers can help to achieve the desirable goal of decreasing the wind energy cost by increasing the efficiency, and thus the energy capture, or by reducing structural loading and increasing the lifetimes of the components and turbine structures [5]. This review paper aims also at sketching the main challenges that exist in the wind industry and to stimulate new research topics in this area. Although wind turbines come in both vertical–axis and horizontal–axis configurations, this work will focus only on horizontal–axis wind turbines, since they represent the most commonly produced large–scale installations today.

Horizontal–axis wind turbines have the advantage that the rotor is placed atop a tall tower, where it can take advantage of larger wind speeds higher above the ground. Moreover, horizontal–axis wind turbines used for utility–scale installations include pitchable blades, improved power capture and structural performance, as well as no need for tensioned cables used to add structural stability [5]. Vertical–axis solutions are more common for smaller turbines, where these disadvantages become less important and the benefits of reduced noise and omni–directionality become more pronounced. Note finally that the generating capacity of modern and commercial turbines ranges from less than 1kW to several MW. The proper wind turbine system modelling oriented to the design of a suitable control strategy is more cost–effective for large wind turbines, and therefore this work will focus on wind turbines with capacities of several MW.

Another important issue derives from the steadily increasing sizes and a growing complexity

of wind turbines, thus giving rise to more severe requirements regarding the system safety, reliability and availability [6]. The safety demand can be commonly achieved by introducing redundancy in the system architecture, like additional sensors, which become vital for a safer operation of wind turbines. The classic example regards the pitch system for adjusting the angles of a rotor blade. For each of the three blades, one totally independent pitch system is used, such that in the worst case of a malfunction in one or two pitch systems, the remaining one or two would still be able to bring the turbine to a standstill. This solution improves the system safety, but it generates additional costs and possibly additional turbine downtimes due to faults in the redundant system parts. The enhanced safety may lead to reduce the system availability.

Even when reducing hardware redundancies, large wind turbines are prone to unexpected malfunctions or alterations of the nominal working conditions. Many of these anomalies, even if not critical, often lead to turbine shutdowns, again for safety reasons. Especially in offshore wind turbines, this may result in a substantially reduced availability, because rough weather conditions may prevent the prompt replacement of the damaged system parts. The need for reliability and availability that guarantees the continuous energy production requires the so–called sustainable control solutions. These schemes enable to keep the turbine in operation in the presence of anomalous situations, perhaps with reduced performance, while managing the maintenance operations. Apart from increasing availability and reducing turbine downtimes, sustainable control schemes might also obviate the need for more hardware redundancy, if virtual sensors could replace redundant hardware sensors [7, 8]. These schemes currently employed in wind turbines are typically on the level of the supervisory control, where commonly used strategies include sensor comparison, model comparison and thresholding tests [7, 8]. These strategies enable safe turbine operations, which involve shutdowns in case of critical situations, but they are not able to actively counteract anomalous working conditions. Therefore, the goal of this work is also to investigate these so–called sustainable control strategies, which allow to obtain a system behaviour that is close to the nominal situation in presence of unpermitted deviations of any characteristic properties or system parameters from standard conditions (*i.e.* a fault) [9]. Moreover, these schemes should provide the reconstruction of the equivalent unknown input that represents the effect of a fault, thus achieving the so–called fault diagnosis task [7, 8].

The rest of this paper is organised as follows. Section 2 describes the configurations and basic operation of wind turbines. Section 3 explains the layout of the wind turbine main control loops, including wind inflow characteristics and available sensors and actuators for use in control. Section 4 describes the current state of wind turbine control, which is then followed by a discussion of advanced control opportunities in Section 5. On the other hand, Section 5.1 outlines the main sustainable control strategies recently proposed for wind turbines. Concluding remarks are finally summarised in Section 6.

2. Wind Turbine Modelling Issues

Prior to apply any new control strategies on a real wind turbine, the efficacy of the control scheme has to be tested in detailed aero–elastic simulation model. Several simulation packages exist that are commonly used in academia and industry for wind turbine load simulation. This paper recalls one of the most used simulation package, that is the Fatigue, Aerodynamics, Structures, and Turbulence (FAST) code [10] provided by NREL, since it represents a reference simulation environment for the development of high–fidelity wind turbine prototypes that are taken as a reference test–cases for many practical studies.

FAST provides a high–fidelity wind turbine model with 24 degrees of freedom, which is appropriate for testing the developed control algorithms but not for control design. For the latter purpose, a reduced–order dynamic wind turbine model, which captures only dynamic effects directly influenced by the control, is recalled in this section and it can be used for model–

based control design. It almost corresponds to the model presented in [5].

The main components of a horizontal-axis wind turbine that are visible from the ground are its tower, nacelle, and rotor, as can be seen in Fig. 2. The nacelle houses the generator, which is driven by the high–speed shaft. The high-speed shaft is in turn usually driven by a gear box, which steps up the rotational speed from the low–speed shaft. The low-speed shaft is connected to the rotor, which includes the airfoil–shaped blades. These blades capture the kinetic energy in the wind and transform it into the rotational kinetic energy of the wind turbine.

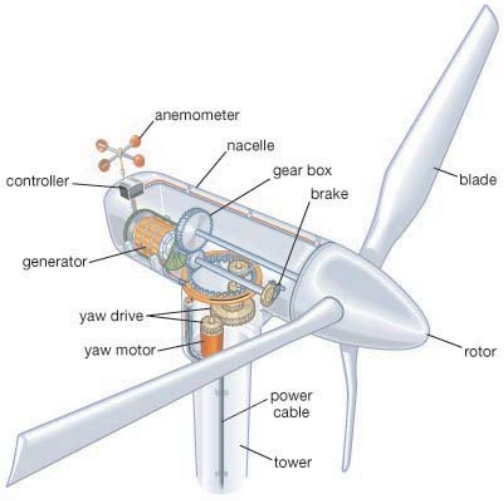

Figure 2. Main wind turbine components.

The complete wind turbine model consists of several submodels for the mechanical structure, the aerodynamics, as well as the dynamics of the pitch system and the generator/ converter system, as sketched in Fig. 3. The generator/converter dynamics are usually described as a first order delay system. However, when the delay time constant is very small, an ideal converter can be assumed, such that the reference generator torque signal is equal to the actual generator torque. In this situation, the generator torque can be considered as a system input.

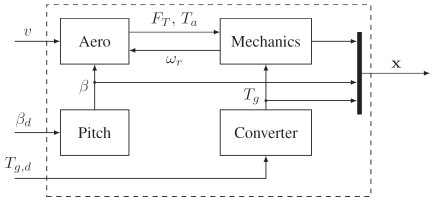

Figure 3. Block diagram of the complete wind turbine model.

Fig. 3 reports also the wind turbine inputs and outputs. In particular, v is wind speed, F_T and T_a correspond to the rotor thrust force and rotor torque, respectively; ω_r is the rotor angular velocity, x the state vector, T_g the generator torque, and $T_{g,d}$ the demanded generator torque. β is the pitch angle, whilst β_d its demanded value.

2.1. Wind Turbine Tower and Blade Models

As an example, a mechanical wind turbine model with four degrees of freedom is considered, since these degrees of freedom are the most strongly affected by the wind turbine control. In particular, the represent the fore–aft tower bending, the flap–wise blade bending, the rotor rotation, and the generator rotation [11].

Both the tower and blade bending are not modelled by means of bending beam models, but only the the translational displacement of the tower top and the blade tip are considered, where the bending stiffness parameters are transformed into equivalent translational stiffness parameters, as depicted in Fig. 4.

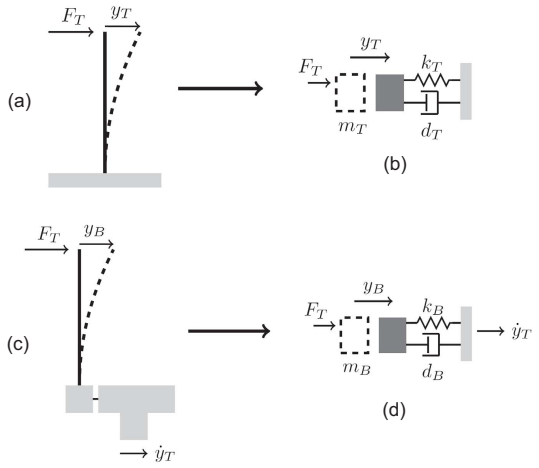

Figure 4. (a) tower bending, (b) mechanical model with spring and damper. (c) blade bending and (d) mechanical model [11].

For the tower, the equivalent translational stiffness parameter is derived by means of a direct stiffness method common in structural mechanics calculations [11].

Since the blades move with the tower, the blade tip displacement is considered in the moving tower coordinate system and the tower motion must be taken into account for the derivation of the kinetic energy of the blade. The force F_T acts both on the tower and on N blades. Only one collective blade degree of freedom is considered. Note that the N blade degrees of freedom would have to be considered individually if control strategies for load reduction involving individual blade pitch control were designed. The assumption that the same external force F_T acts on both the tower and the blade degrees of freedom (with N blades) is a simplification. It is reasonable, however, because the rotor thrust force, which is caused by the aerodynamic lift forces acting on the blade elements, acts on the tower top, thus causing a distributed load on each blade. This distributed load generates a bending of the blade, which could be modelled as a bending beam. A beam subjected not to a distributed load but to a concentrated load at the upper point must have a higher bending beam stiffness, in order that the same displacement results at the upper point. However, a reduced–order wind turbine model considers only the blade tip displacement, which requires the assumption of a translational stiffness. To obtain an adequate translational stiffness constant, the bending stiffness of the bending beam must thus be larger than the case of a distributed load.

On the other hand, the drivetrain consisting of rotor, shaft and generator is modelled as a two–mass inertia system, including shaft torsion, where the two inertias are connected with a torsional spring with spring constant k_S and a torsional damper with damping constant d_S, as illustrated in Fig. 5.

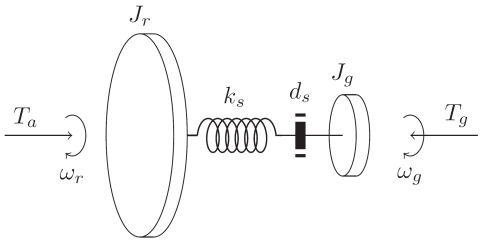

Figure 5. Model of the drivetrain [11].

With reference to Fig. 5, the angular velocities ω_r and ω_g are the time derivatives of the rotation angles θ_r and θ_g. In this case, the rotor torque T_a is generated by the lift forces on the individual blade elements, whilst T_g represents the generator torque. The ideal gearbox effect can be simply included in the generator model by multiplying the generator inertia J_g by the square of the gearbox ratio n_g.

The motion equations are derived by means of Lagrangian dynamics, which first requires to define the generalised coordinates and generalised external forces. In this way, the energy terms of the system are derived, as well as the motion equations. The vector of generalised coordinates is given by: $\mathbf{q} = [y_T,\, y_B,\, \theta_r,\, \theta_g]^T$, whilst the vector of external forces is defined as $\mathbf{f} = [F_T,\, F_T,\, T_a,\, -T_g]$.

The generalised force F_T represents the rotor thrust force, which can be computed from the wind speed at the blade and from the aerodynamic map of the thrust coefficient. On the other hand, the generalised force T_a is given by the aerodynamic rotor torque, which can be calculated from the wind speed and from the aerodynamic map of the torque coefficient described in Section 2.4. By considering the tower dynamics, the complete blade tip displacement is given by $y_T + y_B$, and the kinetic energy has the following form:

$$E_K = \frac{1}{2}\, m_T\, \dot{y}_T^2 + \frac{1}{2}\, N\, m_B\, (\dot{y}_T + \dot{y}_B)^2 + \frac{1}{2}\, J_r \dot{\theta}_r^2 + \frac{1}{2}\, J_g\, \dot{\theta}_g^2 \tag{1}$$

In the same way, the potential energy has the form:

$$E_P = \frac{1}{2}\, k_T\, y_T^2 + \frac{1}{2}\, N\, k_B\, y_B^2 + \frac{1}{2}\, k_S \left(\theta_r - \frac{1}{n_g}\, \theta_g\right)^2 \tag{2}$$

with n_g the gearbox ratio. The dampings in the system produce generalised friction forces, which can be written as derivatives of a quadratic form, *e.g.* the dissipation function. In this case, it assumes the form:

$$P_D = \frac{1}{2}\, d_T\, \dot{y}_T^2 + \frac{1}{2}\, N\, d_B\, \dot{y}_B^2 + \frac{1}{2}\, d_S \left(\dot{\theta}_r - \frac{1}{n_g} \dot{\theta}_g\right)^2 \tag{3}$$

The Lagrangian equations of second order including the dissipation term are given by:

$$\frac{d}{dt}\left(\frac{\partial L}{\partial \dot{q}_i}\right) - \frac{\partial L}{\partial q_i} = f_i - \frac{\partial P_D}{\partial \dot{q}_i} \tag{4}$$

where the Lagrangian function L denotes the difference between kinetic and potential energy. As the kinetic energy in (1) does not depend on the generalised coordinates and the potential

energy in (2) does not depend on the generalised velocities, the motion equations in the following form are obtained:

$$\left\{\begin{array}{rcl} (m_T + N\,m_B)\,\ddot{y}_T + N\,m_B\,\ddot{y}_B + d_T\,\dot{y}_T + k_T\,y_T &=& F_T \\ N\,m_B\,\ddot{y}_T + N\,m_B\,\ddot{y}_B + N\,dB\,\dot{y}_B + N\,k_B\,y_B &=& F_T \\ J_r\,\ddot{\theta}_r + d_S\left(\omega_r - \frac{1}{n_g}\,\omega_g\right) + k_S\left(\theta_r - \frac{1}{n_g}\,\theta_g\right) &=& T_a \\ J_r\,\frac{1}{n_g}\,\ddot{\theta}_g - d_S\left(\omega_r - \frac{1}{n_g}\,\omega_g\right) - k_S\left(\theta_r - \frac{1}{n_g}\,\theta_g\right) &=& -T_g \end{array}\right. \tag{5}$$

The system (5) can be rewritten in matrix form as:

$$\mathbf{M}\,\ddot{q} + \mathbf{D}\,\dot{q} + \mathbf{K}\,q = \mathbf{f} \tag{6}$$

where the mass matrix $\mathbf{M}$, the damping matrix $\mathbf{M}$ and the stiffness matrix $\mathbf{K}$ have the form:

$$\begin{array}{l} \mathbf{M} = \left[\begin{array}{cccc} m_T + N\,m_B & N\,m_B & 0 & 0 \\ N\,m_B & N\,m_B & 0 & 0 \\ 0 & 0 & J_r & 0 \\ 0 & 0 & 0 & J_g \end{array}\right], \quad \mathbf{D} = \left[\begin{array}{cccc} d_T & 0 & 0 & 0 \\ 0 & N\,d_B & 0 & 0 \\ 0 & 0 & d_S & -\frac{d_S}{n_g} \\ 0 & 0 & -\frac{d_S}{n_g} & \frac{d_S}{n_g^2} \end{array}\right] \\ \mathbf{K} = \left[\begin{array}{cccc} k_T & 0 & 0 & 0 \\ 0 & N\,k_B & 0 & 0 \\ 0 & 0 & k_S & -\frac{k_S}{n_g} \\ 0 & 0 & -\frac{k_S}{n_g} & \frac{k_S}{n_g^2} \end{array}\right] \end{array} \tag{7}$$

The second order system of differential equations (6) can be transformed into a first order state–space model by introducing the state vector $x = [q,\, \dot{q}]^T$. To this aim, the expression (6) is solved with respect to the second time derivative of the coordinate vector $\mathbf{q}$. The equivalent state–space model is thus obtained in the form:

$$\left\{\begin{array}{rcl} \dot{\mathbf{x}} &=& \mathbf{A}_m\,\mathbf{x} + \mathbf{B}_m\,\mathbf{u}_m \\ \mathbf{y} &=& \mathbf{C}_m\,\mathbf{x} \end{array}\right. \tag{8}$$

where the state vector is given by $\mathbf{x} = \left[y_T,\, y_B,\, \theta_r,\, \theta_g,\, \dot{y}_T,\, \dot{y}_B,\, \dot{\theta}_r,\, \dot{\theta}_g\right]^T$, the input vector is $\mathbf{u}_m = [F_T,\, T_a,\, T_g]^T$, whilst the system matrices have the form:

$$\mathbf{A}_m = \left[\begin{array}{cc} 0_{4\times4} & I_{4\times4} \\ -\mathbf{M}^{-1}\,\mathbf{K} & -\mathbf{M}^{-1}\,\mathbf{D} \end{array}\right], \quad \mathbf{B}_m = \left[\begin{array}{c} 0_{4\times3} \\ \mathbf{M}^{-1}\,\mathbf{Q} \end{array}\right], \quad \mathbf{C}_m = \mathbf{I}_{8\times8}, \quad \text{with } \mathbf{Q} = \left[\begin{array}{ccc} 1 & 0 & 0 \\ 1 & 0 & 0 \\ 0 & 1 & 0 \\ 0 & 0 & -1 \end{array}\right] \tag{9}$$

2.2. Pitch Model

In pitch–regulated wind turbines, the pitch angle of the blades is controlled only in the full load region to reduce the aerodynamic rotor torque, thus maintaining the turbine at the desired rotor speed. Moreover, the pitching of the blades to feather position (*i.e.* 90^o) is used as main braking system to bring the turbine to standstill in critical situations. Two different types of pitch technologies are usually exploited in wind turbines, *i.e.* hydraulic and electromechanical pitch systems. For hydraulic pitch systems, the dynamics can be modelled by means of a second–order delay model [6], which is able to display oscillatory behaviour. For electromechanical pitch

systems, which are more commonly used, a first–order delay model is sufficient. In this work, the first–order delay model is recalled:

$$\dot{\beta} = -\frac{1}{\tau}\,\beta + \frac{1}{\tau}\,\beta_d \tag{10}$$

where β and β_d are the physical and the demanded pitch angle, respectively. The parameter τ denotes the delay time constant.

2.3. Generator/Converter Dynamic Model

An explicit model for the generator/converter dynamics can be included into the complete wind turbine system model. Note that for mere simulation purposes, this is not necessary, since the generator/converter dynamics are relatively fast. However, when advanced control designs are considered, an explicit generator/converter model might be required in order to take into account generator torque fast dynamics. In this case, a simple first order delay model can be sufficient, as described *e.g.* in [6]:

$$\dot{T}_g = -\frac{1}{\tau_g}\,T_g + \frac{1}{\tau_g}\,T_{g,d} \tag{11}$$

where $T_{g,d}$ represents the demanded generator torque, whilst τ_g the delay time constant.

2.4. Aerodynamic Model

The aerodynamic submodel consists of the expressions for the thrust force F_T acting on the rotor and the aerodynamic rotor torque T_a. They are determined by the reference force F_{st} and by the aerodynamic rotor thrust and torque coefficients C_T and C_Q:

$$\begin{cases} F_T &= F_{st}\,C_T\,(\lambda,\,\beta) \\ T_a &= F_{st}\,R\,C_Q\,(\lambda,\,\beta) \end{cases} \tag{12}$$

The reference force F_st is defined from the impact pressure $\frac{1}{2}\,\rho\,v^2$ and the rotor swept area $\pi\,R^2$ (with rotor radius R), where ρ denotes the air density:

$$F_{st} = \frac{1}{2}\,\rho\,\pi\,R^2\,v^2 \tag{13}$$

It is worth noting that for simulation purpose, the static wind speed v is used. However, a more accurate model should exploit the effective wind speed $v_e = v - (\dot{y}_T + \dot{y}_B)$, *i.e.* the static wind speed corrected with by the tower and blade motion effects. However, the aerodynamic maps used for the calculation of the rotor thrust and torque are usually represented as static 2–dimensional tables, which already take into account the dynamic contributions of both the tower and the blade motions.

As highlighted in the expressions (12), the rotor thrust and torque coefficients (C_T, C_Q) depend on the tip speed ratio $\lambda = \frac{\omega_r\,R}{v}$ and the pitch angle β. Therefore, the rotor thrust F_T and torque T_a assume the following expressions:

$$\begin{cases} F_T &= \frac{1}{2}\,\rho\,\pi\,R^2\,C_T\,(\lambda,\,\beta)\;v^2 \\ T_a &= \frac{1}{2}\,\rho\,\pi\,R^3\,C_Q\,(\lambda,\,\beta)\;v^2 \end{cases} \tag{14}$$

The expressions (14) highlight that the rotor thrust F_T and torque T_a are nonlinear functions dependent on the wind speed v, the rotor speed ω_r, and the pitch angle β. These functions are usually expressed as two–dimensional maps, which must be known for the whole range

of variation of both the pitch angles and tip speed ratios. These maps are usually a static approximation of more detailed aerodynamic computations that can be obtained using for example the Blade Element Momentum (BEM) method. In this case, the aerodynamic lift and drag forces at each blade section are calculated and integrated in order to obtain the rotor thrust and torque.

It is worth noting that for simulation purposes, the tabulated versions of the aerodynamic maps C_Q and C_T are sufficient. On the other hand, for control design, the derivatives of the rotor torque (and thrust) are needed, thus requiring a description of the aerodynamic maps as analytical functions. Therefore, these maps can be approximated using combinations of polynomial and exponential functions, whose powers and coefficients are estimated via *e.g.* identification [12] approaches.

2.5. Wind Turbine Overall Model

By replacing the expressions (14) for the rotor thrust and torque into the mechanical model (8) and adding the models (10) and (11) for the pitch and the generator/converter dynamics, a nonlinear state–space model is obtained:

$$\begin{cases} \dot{\mathbf{x}} &= \mathbf{A}\,\mathbf{x} + \mathbf{B}\,\mathbf{u} + g\,(\mathbf{x},\, v) \\ \mathbf{y} &= \mathbf{C}\,\mathbf{x} \end{cases} \tag{15}$$

with a state vector that now includes the pitch angle and the generator torque: $\mathbf{x} = \left[y_T,\, y_B,\, \theta_r - \theta_g,\, \dot{y}_T,\, \dot{y}_B,\, \dot{\theta}_r,\, \dot{\theta}_g,\, \beta\right]^T$. Since the rotor thrust force and the rotor torque have been used as inputs for the vector $\mathbf{u}_m$ in the mechanical submodel (8), a new input vector is defined for the complete state–space model (15), *i.e.* $\mathbf{u} = [\beta_d,\, T_g]^T$, whose components are the demanded pitch angle and the generator torque, respectively. The wind speed is normally considered as a disturbance input. The linear part of the state–space model (15) is defined by the matrices:

$$\mathbf{A} = \begin{bmatrix} 0_{3\times3} & \tilde{\mathbf{L}} & 0_{3\times1} & 0_{3\times1} \\ \mathbf{M}^{-1}\,\tilde{\mathbf{K}} & \mathbf{M}^{-1}\,\mathbf{D} & 0_{4\times1} & \begin{bmatrix} 0_{3\times1} \\ -\frac{1}{J_g} \end{bmatrix} \\ 0_{1\times3} & 0_{1\times4} & -\frac{1}{\tau} & 0 \\ 0_{1\times3} & 0_{1\times4} & 0 & -\frac{1}{\tau_g} \end{bmatrix}, \quad \mathbf{B} = \begin{bmatrix} 0_{7\times1} & 0_{7\times1} \\ \frac{1}{\tau} & 0 \\ 0 & -\frac{1}{\tau_g} \end{bmatrix} \tag{16}$$

with:

$$\tilde{\mathbf{L}} = \begin{bmatrix} 1 & 0 & 0 & 0 \\ 0 & 1 & 0 & 0 \\ 0 & 0 & 1 & -1 \end{bmatrix} \quad \text{and} \quad \tilde{\mathbf{K}} = \begin{bmatrix} k_T & 0 & 0 \\ 0 & N\,k_B & 0 \\ 0 & 0 & k_S \\ 0 & 0 & -k_S \end{bmatrix} \tag{17}$$

Moreover, the system vector in (15) nonlinearly depends on the state and input vector:

$$g\,(\mathbf{x},\, v) = \begin{bmatrix} 0_{4\times1} \\ \frac{1}{m_B}\,F_T\,(\mathbf{x},\, v) \\ \frac{1}{J_r}\,T_a\,(\mathbf{x},\, v) \\ 0_{3\times1} \end{bmatrix} \tag{18}$$

Here, the rotor thrust and torque expressions are given in (14), whilst the mass and damping matrices are defined in (7).

It is worth noting that in a real wind turbine, the centrifugal forces acting on the rotating rotor blades lead to a stiffening of the blades. As a consequence, the bending behaviour of the

rotor blades depends on the rotor speed itself. By considering again the translational spring–mass system of the blade–tip displacement, this second–order effect can be included in the model (15) by introducing a translational blade stiffness parameter k_B dependent on the rotor speed, *i.e.* $k_B(\omega_r) = \alpha\, m_B\, r_B\, \omega_r^2$. r_B denotes the distance from the blade root to the blade centre of mass and α tuning parameter. In this way, by including the centrifugal stiffening correction, the nonlinear system vector $g(\mathbf{x},\, v)$ in (18) has the form:

$$g(\mathbf{x},\, v) = \begin{bmatrix} 0_{3\times 1} \\ \frac{N}{m_T}\, k_B(\omega_r)\, y_B \\ \frac{1}{N\, m_B}\, F_T(\mathbf{x},\, v) + \frac{m_T + N\, m_B}{m_T\, m_B}\, k_B(\omega_r)\, y_B \\ \frac{1}{J_r}\, T_a(\mathbf{x},\, v) \\ 0_{3\times 1} \end{bmatrix} \tag{19}$$

The inclusion of the centrifugal term is inspired from the FAST code, in order to obtain a high–fidelity wind turbine simulation model. For example, the translational blade bending model could be required when overspeed scenarios shall be taken into account. However, for the usual operating regimes of a wind turbine, the corrections induced by the centrifugal blade stiffening have only minor effects on the final results. Therefore, the centrifugal correction has been recalled here for the sake of completeness, but it has limited interest in real cases.

2.6. Measurement Errors

Wind turbine high–fidelity simulators, which were described for example in [6, 13], consider white noise added to all measurements. This relies on the assumption that noisy sensor signals should represent more realistic scenarios. However, this is not the case, as a realistic simulation would require an accurate knowledge of each sensor and its measurement reliability. To the best of the authors' knowledge and from their experience with wind turbine systems, all main measurements acquired from the wind turbine process (rotor and generator speed, pitch angle, generator torque), are virtually noise–free or affected by very weak noise.

3. Wind Turbine Control Strategies

Wind turbine control goals and strategies are affected by turbine configuration. Horizontal–axis wind turbine may be "upwind", with the rotor on the upwind side of the tower, or "downwind". The choice of upwind versus downwind configuration affects the choice of yaw controller and the turbine dynamics, and thus the structural design. Wind turbines may also be variable pitch or fixed pitch, meaning that the blades may or may not be able to rotate along their longitudinal axes. Although fixed–pitch machines are less expensive initially, the reduced ability to control loads and change the aerodynamic torque means that they are becoming less common within the realm of large wind turbines. Variable-pitch turbines may allow all or part of their blades to rotate along the pitch axis.

Moreover, wind turbines can be variable speed or fixed speed. Variable–speed turbines tend to operate closer to their maximum aerodynamic efficiency for a higher percentage of the time, but require electrical power processing so that the generated electricity can be fed into the electrical grid at the proper frequency. As generator and power electronics technologies improve and costs decrease, variable–speed turbines are becoming more popular than constant–speed turbines at the utility scale.

Fig. 6 shows an example power curve for a variable–speed wind turbine. When the wind speed is low (usually below 6 m/s), the power available in the wind is low compared to losses in the turbine system so the turbine is not running. This operational region is sometimes known as Region 1. When the wind speed is high, Region 3 (above 11.7 m/s), power is limited to avoid exceeding safe electrical and mechanical load limits.

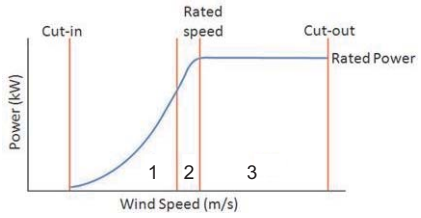

Figure 6. Example of wind turbine power curve.

The main difference between fixed–speed and variable speed wind turbines appears for mid–range wind speeds, the Region 2 in Fig. 6 , which normally encompasses wind speeds between 6 and 11.7 m/s. Except for one design operating point (10 m/s), a variable–speed turbine captures more power than a fixed–speed turbine. The reason for the discrepancy is that variable–speed turbines can operate at maximum aerodynamic efficiency over a wider range of wind speeds than fixed–speed turbines. The maximum difference between the generated power of the two wind turbines in Region 2 can be about 150 kW.

For typical wind speed situations, the variable–speed turbine can capture 2.3% more energy per year than the constant–speed turbine, which is considered to be a significant difference in the wind industry. Not shown in Fig. 6 is the "high wind cut–out", a wind speed above which the turbine is powered down and stopped to avoid excessive operating loads. High wind cut–out typically occurs at wind speeds above 20 – 30 m/s for large turbines, with many factors determining the exact value. Even a perfect wind turbine cannot fully capture the power available in the wind. In fact, actuator disc theory shows that the theoretical maximum aerodynamic efficiency, which is called the Betz Limit, is approximately 60% of the wind power. The reason that an efficiency of 100% cannot be achieved is that the wind must have some kinetic energy remaining after passing through the rotor disc. If it did not, the wind would by definition be stopped and no more wind would be able to pass through the rotor to provide energy to the turbine.

In designing controllers for wind turbines, it is often assumed (as in (14)) that the wind speed is uniform across the rotor plane. However, as indicated by the "instantaneous wind field" in Fig. 7, the wind input can vary substantially in space and time as it approaches the rotor plane. The deviations of the wind speed from the expected nominal wind speed across the rotor plane are considered disturbances for control design. It is virtually impossible to obtain a good measurement of the wind speed encountering the blades because of the spatial and temporal variability and also because the rotor interacts with and changes the wind input. Not only does turbulent wind cause the wind to be different for the different blades, but the wind speed input is different at different positions along each blade. Utility–scale wind turbines have several levels of control, which can be called "supervisory control", "operational control", and "subsystem control".

The top–level supervisory control determines when the turbine starts and stops in response to changes in the wind speed, and also monitors the health of the turbine. The operational control determines how the turbine achieves its control objectives in Regions 2 and 3. The subsystem controllers cause the generator, power electronics, yaw drive, pitch drive, and other actuators to perform as desired. In this section, the operational control loops and the controllers shown in Fig. 7, which exploit the submodels described in Section 2. In particular, the main control objectives, which are recalled in Section 3.1, will be exploited for illustrating the pitch and torque controllers in Section 4.

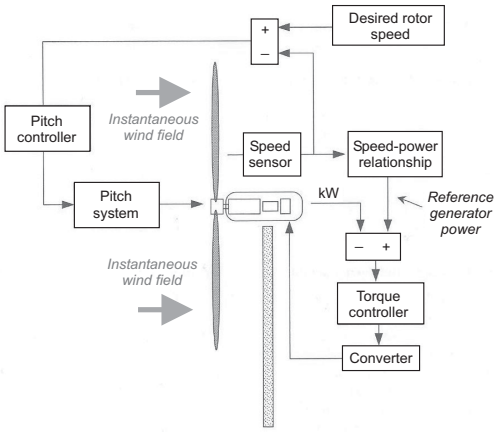

Figure 7. Block diagram of the wind turbine control loops.

3.1. Control Loops and Objectives

The primary Region 2 control objective for a variable–speed wind turbine is to maximise the power coefficient, and in particular the C_Q map in (12). As already shown in Section 2.4, this power coefficient is a function of the turbine s tip–speed ratio λ, which is defined in Section 2.4. Thus, the tip–speed ratio is the ratio of the linear (tangential) speed of the blade tip to the wind speed, v is always time-varying, and ω_r is time–varying for a variable–speed turbine. The relationship between C_Q and the tip–speed ratio λ is a turbine–specific nonlinear function. As already discussed, C_Q also depends on the blade pitch angle in a nonlinear fashion, and these relationships have the same basic shape for most modern wind turbines. An example of C_Q surface is shown in Fig. 8 for a generic wind turbine.

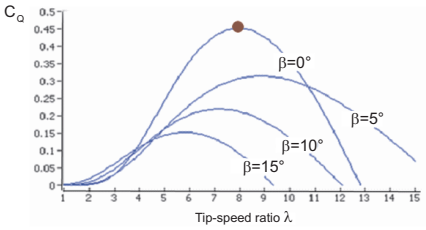

Figure 8. Example of power coefficient curve.

As shown in Fig. 8, the turbine will operate at its highest aerodynamic efficiency point, $C_{\max}$, at a certain pitch angle and tip–speed ratio. The pitch angle is easy to control, and can be reliably maintained at the optimal efficiency point. However, the tip–speed ratio depends on the incoming wind speed v and therefore is constantly changing. Thus, the Region 2 control is primarily concerned with varying the turbine speed to track the wind speed. Section 4 will explain how this control objective can be achieved.

On utility–scale wind turbines, Region 3 control is typically performed via a separate pitch control loop, as shown in Fig. 3 of Section 2. In the Region 3, the primary objective is to limit the turbine power so that safe electrical and mechanical loads are not exceeded. Power limitation can be achieved by pitching the blades or by yawing the turbine out of the wind, both of which can reduce the aerodynamic torque below what is theoretically available from an

increase in wind speed. Note that the power P is related to rotor speed ω_r and aerodynamic torque T_a by the relation:

$$P = T_a \, \omega_r \tag{20}$$

If the power and rotor speed are held constant, the aerodynamic torque must also be constant even as wind speed varies. It is desirable to produce as much power as the turbine can safely produce, the limit of which is known as the turbine s rated power. In the Region 3, the pitch control loop regulates the rotor speed ω_r (at the turbine s "rated speed") so that the turbine operates at its rated power.

It is worth noting that the wind turbine blades may be controlled to all turn collectively or to each turn independently or individually. As outlined in Section 2.2, suitable pitch systems can be used to change the aerodynamic torque from the wind input, and are often fast enough to be of interest to the control community. Typical maximum pitch rates range from 18 deg/s for 600 kW research turbines down to 8 deg/s for 5 MW turbines. Variable–pitch turbines can limit power either by pitching to "stall" or to "feather", and fixed–pitch turbines typically limit power by entering the aerodynamic stall regime above rated wind speed. A blade in full feather is one in which the leading edge of the blade points directly into the wind. A discussion of the benefits of pitching to feather versus pitching to stall is outside the scope of this review paper, but more information can be found *e.g.* in [5].

4. Feedback Controls for Wind Turbines

This section provides further information regarding what control strategies are typically used for the torque control and the pitch control blocks in Fig. 3 of Section 2. As depicted in Fig. 3, both control loops typically only use rotor speed feedback. The other sensors and measurements acquired from the wind turbine can be used for advanced control purposes, as outlined in Section 5.1.

As shown in Fig. 6, the nominal operating trajectory of the wind turbine is created to satisfy different demands below and above a certain wind speed. Since the classical control approach deals only with SISO transfer functions, and because several references exist, the control task is split into the design of multiple separate compensators. The design of the complete wind turbine controller is thus divided into four main control boxes and design steps, as listed below:

(i) Controller operating in partial load condition: it refers to the design of the generator torque controller. This controller operates in the partial load (Region 2), and should maximise the energy production while minimising mechanical stress and actuator usage;

(ii) Controller operating in full load condition: it concerns the speed controller and power controller. These controllers operate in the full load (Region 3), and should track the rated generator speed and limiting the output power;

(iii) Bumpless transfer: it describe the design of the mechanism that eliminates bumps on the control signals, when switching between the controllers in the partial load and full load regions;

(iv) Structural stress damper: it regards the design of structure and drivetrain stress damper. The purpose of the module is to dampen drivetrain oscillations and reduce structural stress that could affect the wind turbine tower.

The first two items are the main control loops, whilst the two other tasks concern advanced control issues, which can enhance both the control and system performances. Note also that the transfer functions outlined throughout this section need to be discretised to allow the implementation of the controllers and filters in real–time conditions. In this way, the overall controller design consists of using two different controllers for the partial load region and the full load region. When the wind speed is below the rated value, the control system should maintain

the pitch angle at its optimal value and control the generator torque in order to achieve the optimal tip–speed ratio (switch to Region 2).

Above the rated wind speed the output power is kept constant by pitching the rotor blades, while using a power controller that manipulates the generator torque around a constant value to remove steady–state errors on the output power. In both regions a drivetrain stress damper is exploited to dampen drivetrain oscillations actively. Together, the two sets of controllers are able to solve the control task of tracking the ideal power curve in Fig. 8. In order to switch smoothly between the two sets of controllers a bumpless transfer mechanism is implemented.

4.1. Partial Load Operation Controller

At low wind speeds, *i.e.* in partial load operation, variable–speed control is implemented to track the optimum point on the C_Q–surface for maximising the power output. The speed of the generator is controlled by regulating the torque on the generator through the generator torque controller. The purpose of this section is to go through the design of the generator torque controller. In partial load operation it is chosen to operate the wind turbine at $\beta = 0^o$ since the maximum power coefficient is obtained at this pitch angle. This means that the highest efficiency is achieved for:

$$\lambda_{\text{opt}} = \frac{\omega_{r,\,\text{opt}}\, R}{v} \tag{21}$$

where λ_{opt} is the tip–speed ratio maximising the C_Q–value for $\beta = 0^o$, and $\omega_{r,\,\text{opt}}$ is the optimum rotor speed. In order to obtain the optimal tip–speed ratio a method is used, which suggests to apply a certain generator torque as a function of the generator speed [14]. The advantage of this approach is that only the measurement of the rotor speed or generator speed is required. When utilising this approach, the controller structure for partial load operation is illustrated in Fig. 9.

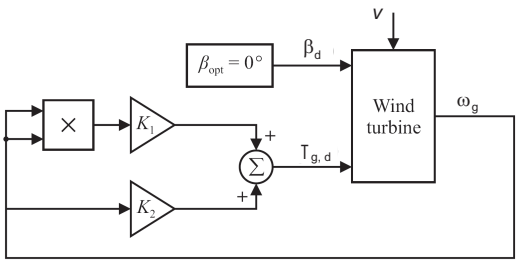

Figure 9. Generator torque controller for operation in partial load region (Region 2).

The principle of the standard control law is to calculate the wind speed in the definition of the tip–speed ratio, and replace it into the expression for the aerodynamic torque in (14). Hence, the relation can be obtained expressing the required generator torque based on the maximum power coefficient and the optimal tip–speed ratio:

$$v(t) = \frac{\omega_r(t)\, R}{\lambda(t)} \tag{22}$$

This expression is inserted into (14) describing the aerodynamic torque:

$$T_a(t) = \frac{1}{2}\,\rho\,\pi\,R^2\,\frac{R^3}{\lambda^3(t)} C_Q\left(\lambda(t),\,\beta(t)\right)\omega_r^2(t) \tag{23}$$

Since the wind turbine includes a transmission system, the gear ratio and friction components of the drivetrain have to be considered when determining the generator torque corresponding to a certain aerodynamic torque. In order to describe the generator torque only as function of the generator speed, the system has to be assumed in steady–state, where $\dot{\omega}_r(t) = \dot{\omega}_g(t) = 0$ and $\omega_g(t) = n_g\,\omega_r(t)$. In this way, by considering the drivetrain equations in (5), the following expression is obtained:

$$T_{g,\,d} = \frac{1}{2}\,\rho\,\pi\,R^2\,\frac{R^3}{n_g^3\,\lambda_{\rm opt}^3}\,C_{\max}\,\omega_g^2(t) - d_S\,\left(\frac{1}{n_g^2} + 1\right)\,\omega_g \tag{24}$$

with:

$$K_1 = \tfrac{1}{2}\,\rho\,\pi\,R^2\,\tfrac{R^3}{n_g^3\,\lambda_{\rm opt}^3}, \quad K_2 = -d_S\,\left(\tfrac{1}{n_g^2} + 1\right) \tag{25}$$

4.2. Full Load Operation Controller

For the high wind speeds, *i.e.* in full load operation, the desired operation of the wind turbine is to keep the rotor speed and the generated power at constant values. The main idea is to use the pitch system to control the efficiency of the aerodynamics while applying the rated generator torque. However, in order to improve tracking of the power reference and cancel steady–state errors on the output power, a power controller is also introduced. Therefore, in this section the design of the speed controller and the power controller is sketched. The structure of the controllers operating above the rated wind speed is shown in Fig. 10.

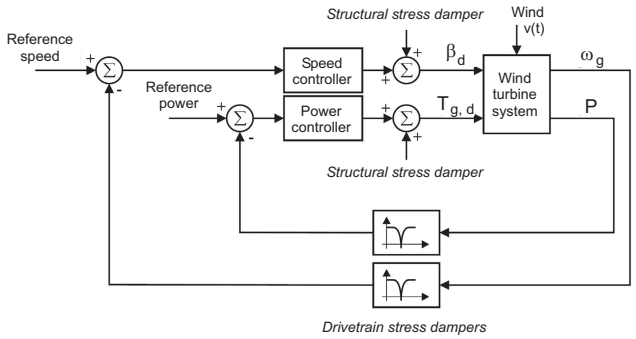

Figure 10. Speed controller and power controller for operation in the full load region (Region 3).

The wind speed is considered the disturbance input to the system. However, higher frequency components such as the resonant frequency of the drive train are also apparent on the measured generator speed. Therefore, the measured generator speed is band–stop filtered before it is fed to the controller, to remove the drivetrain eigenfrequency from the measurement. This solution is also found in other wind turbine control schemes to mitigate the effects of structural oscillations, by injecting suitable signals in the control loops. In the following, the design of the speed controller and the power controller is presented.

With reference to the speed controller of Fig. 10, it is implemented as a PI controller that is able to track the speed reference and cancel possible steady–state errors on the generator speed. The speed controller transfer function $D_s(s)$ has the form:

$$D_s(s) = K_{ps}\left(1 + \frac{1}{T_{is}}\,\frac{1}{s}\right) \tag{26}$$

where K_{ps} is the PI proportional gain and T_{is} is the reset rate of the integrator. It can be shown that pitching the blades has a larger influence on the aerodynamic torque at higher wind speeds. For this reason, the gain K_{ps} of the speed controller should be large near the rated wind speed but smaller at higher wind speeds. The optimal gain of the speed controller associated with a certain wind speed can make the system become unstable at higher wind speeds due to the increasing gain of the system. Therefore, the speed controller is configured with one set of parameters in the region corresponding to stationary wind speeds in the interval $12 - -15$ m/s, while a smaller gain is utilised for the region covering wind speeds of $15 - -25$ m/s. Although the system has different gains in these two working regions, it is possible to design the controllers so that similar transient responses of the controlled system are obtained.

On the other hand, with reference to the power controller of Fig. 10, it is implemented again in order to cancel possible steady–state errors on the output power. This suggests using slow integral control for the power controller, as this will eventually cancel steady–state errors on the output power without interfering with the speed controller. However, it may be beneficial to make the power controller faster to improve accuracy in the tracking of the rated power. The power controller is realized as a PI controller, whose transfer function $D_p(s)$ has the form:

$$D_p(s) = K_{pp}\left(1 + \frac{1}{T_{ip}}\frac{1}{s}\right) \tag{27}$$

where K_{pp} is the proportional gain of the PI regulator, whilst T_{ip} is the reset rate of the integrator. By exploiting the measured output power directly can be a problem, since the measurement is very noisy. This means that the measurement noise has to be take into account in the design and yields that the proportional gain has to be sufficiently small. The proportional gain is usually chosen using a trial and error approach while the reset rate is selected large enough to avoid overshoot on the step response.

4.3. Structural and Drivetrain Stress Damper

Active stress damping solutions are deployed in large horizontal–axis wind turbines to mitigate fatigue damage due to drivetrain and structural oscillations and vibrations. The idea is to add proper components to the wind turbine control signals to compensate for the oscillations in the drivetrain and the tower vibrations. These signals should have frequencies equal to the eigenfrequencies of the drivetrain and the wind turbine structure, which can be found by filtering the measurement of the generator speed and the generated power. When the outputs from these filters are added to the generator torque and the pitch command, the phase of the filters must be zero at the resonant frequency to achieve the desired damping effects. These oscillation and vibration dampers are thus implemented to add compensating signals, as shown in Fig. 10.

Second order filter structures for the stress and the structural damping have been proposed and can be applied to dampen the eigenfrequency of both the drivetrain and the tower structure [5]. In general, the filter time constant introduces a zero in the filter that can be used to compensate for time lags in the system. To determine the gain of the filter, the root loci are plotted for the transfer functions from the wind turbine inputs to its outputs. More details on the design of these filters, which are beyond the scope of this paper, can be found in [5].

Note that, due to the higher loads at higher wind speeds, it is favourable if the filter gains depend on the point of operation. A simple way of fulfilling this property is to apply different gains in the partial and full load configurations of the wind turbine controller. Therefore, a bumpless transfer mechanism must ensure that no bumps exist on the control signals in the switch between two different controllers.

5. Advanced Control of Wind Turbines

There are many aspects of wind turbine performance that can be improved with more advanced control development. Researchers have developed methods for using adaptive control to compensate for unknown or time–varying parameters [15]. Other researchers have also begun to investigate the addition of feed-forward control to improve the disturbance rejection performance when the incoming wind profile deviates from that expected [16]. Most of these feed-forward controllers use estimates of the disturbance (or wind deviation). New sensing technologies will enable various avenues of advanced control research. For instance, there has been recent interest in evaluating the potential of LIDAR (which stands for "LIght Detection And Ranging") sensors for wind turbine control [16]. LIDAR is a remote optical sensing technology that has been used since the 1970s for meteorology for measuring wind speed profiles for monitoring hurricanes and wind conditions around airports. New lidar systems based on solid–state sources and off–the–shelf telecommunications equipment allow for inexpensive deployment, modularity, and improved reliability. Depending on the particular type of technology used, lidar sensors can provide quantities representing the wind speed and direction and various wind turbulence and shear parameters. An accurate measurement of the wind profile over the entire rotor plane in Fig. 7 can enable feed-forward pitch control and feed-forward torque control to improve performance dramatically. Advanced wind turbine controllers are further discussed and compared in [4, 16]. As turbines get larger and blades get longer, it is possible that turbine manufacturers will build turbines that allow for different pitch angles at different radial positions along the blades relative to the standard blade twist angle. In this case, separate actuators and controllers may be necessary, opening up even more control opportunities [16].

Note finally that, the need of advanced control solutions for these very demanding systems, motivated also the requirement of reliability, availability, maintainability, and safety over power conversion efficiency. These issues have begun to stimulate research and development of the so–called sustainable control, which is outlined in Section 5.1.

5.1. Sustainable Control Issues

In general, wind turbines in the megawatt size are expensive, and hence their availability and reliability must be high in order to maximise the energy production. This issue could be particularly important for offshore installations, where Operation and Maintenance (O & M) services have to be minimised, since they represent one of the main factors of the energy cost. The capital cost, as well as the wind turbine foundation and installation determine the basic term in the cost of the produced energy, which constitute the energy 'fixed cost'. The O & M represent a 'variable cost' that can increase the energy cost up to about the 30%. At the same time, industrial systems have become more complex and expensive, with less tolerance for performance degradation, productivity decrease and safety hazards. This leads also to an ever increasing requirement on reliability and safety of control systems subjected to process abnormalities and component faults. As a result, it is extremely important the Fault Detection and Diagnosis (FDD) or the Fault Detection and Isolation (FDI) tasks, as well as the achievement of fault–tolerant features for minimising possible performance degradation and avoiding dangerous situations. With the advent of computerised control, communication networks and information techniques, it makes possible to develop novel real–time monitoring and fault–tolerant design techniques for industrial processes, but brings challenges.

In the last years, many works have been proposed on wind turbine FDI/FDD, and the most relevant are *e.g.* in [6]. On the other hand, regarding the FTC problem for wind turbines, it was recently analysed with reference to an offshore wind turbine benchmark *e.g.* in [6]. In general, FTC methods are classified into two types, *i.e.* Passive Fault Tolerant Control (PFTC) scheme and Active Fault Tolerant Control (AFTC) scheme [17]. In PFTC, controllers are fixed and are designed to be robust against a class of presumed faults. In contrast to PFTC, AFTC reacts to

the system component failures actively by reconfiguring control actions so that the stability and acceptable performance of the entire system can be maintained. In particular for wind turbines, FTC designs were considered and compared in [6]. These processes are nonlinear dynamic systems, whose aerodynamics are nonlinear and unsteady, whilst their rotors are subject to complicated turbulent wind inflow fields driving fatigue loading. Therefore, the so–called wind turbine 'sustainable' control represents a complex and challenging task [18].

Therefore, the purpose of this section is outline the basic solutions to sustainable control design, which are able of handling faults affecting the controlled wind turbine. For example, changing dynamics of the pitch system due a fault cannot be accommodated by signal correction. Therefore, it should be considered in the controller design, to guarantee stability and a satisfactory performance. Among the possible causes for changed dynamics of the pitch system, they can due to a change in the air content of the hydraulic system oil. This fault is considered since it is the most likely to occur, and since the reference controller becomes unstable when the hydraulic oil has a high air content. Another issue raises when the generator speed measurement is unavailable, and the controller should rely on the measurement of the rotor speed, which is contaminated with much more noise than the generator speed measurement. This makes it necessary to reconfigure the controller to obtain a reasonable performance of the control system.

Section 5.2 outlines the main differences between active and passive fault–tolerant control systems and suggests how they are applied to the considered system.

5.2. Active and Passive Fault–Tolerant Control Systems

In order to outline and compare the controllers developed using active and passive fault–tolerant design approaches, they should be derived using the same procedures in the fault–free case. In this way, any differences in their performance or design complexity would be caused only by the fault tolerance approach, rather than the underlying controller solutions. Furthermore, the controllers should manage the parameter–varying nature of the wind turbine along its nominal operating trajectory caused by the aerodynamic nonlinearities. Usually, in order to comply with these requirements, the controllers are usually designed for example using Linear Parameter–Varying (LPV) modelling or fuzzy descriptions [5].

The two fault–tolerant control solutions have different structures as shown in Fig. 11. Note that only the active fault–tolerant controller (AFTC) relies on a fault diagnosis algorithm (FDD). This represents the main difference between the two control schemes.

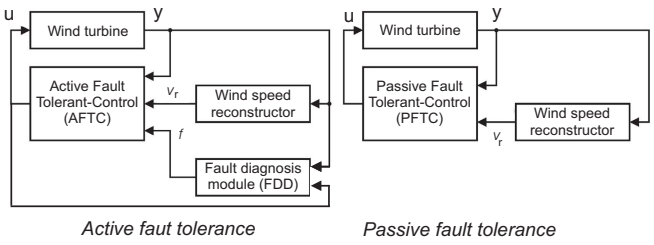

Figure 11. Structures of the active and passive fault–tolerant control systems.

The main point between AFTC and PFTC schemes is that an active fault–tolerant controller relies on a fault diagnosis system, which provides information about the faults f to the controller. In the considered case the fault diagnosis system FDD contains the estimation of the unknown input (fault) affecting the system under control. The knowledge of the fault f allows the AFTC to reconfigure the current state of the system. On the other hand, the FDD is able to improve the controller performance in fault–free conditions, since it can compensate *e.g.* the modelling

errors, uncertainty and disturbances. On the other hand, the PFTC scheme does not rely on a fault diagnosis algorithm, but is designed to be robust towards any possible faults. This is accomplished by designing a controller that is optimised for the fault–free situation, while satisfying some graceful degradation requirements in the faulty cases. However, with respect to the robust control design, the PFTC strategy provides reliable controllers that guarantee the same performance with no risk of false FDI or reconfigurations.

In general, the methods used in the fault–tolerant controller designs should rely on output feedback, since only part of the state vector is measured. Additionally, they should take the measurement noise into account. Moreover, the design methods should be suited for nonlinear systems or linear systems with varying parameters. The latest proposed solutions for the derivation of both active and the passive fault–tolerant controllers rely on LPV and fuzzy descriptions, to which the fault–tolerance properties are added, since these frameworks methods are able to provide stability and guaranteed performance with respect to parameter variations, uncertainty and disturbance. Additionally, LPV and fuzzy controller design methods are well–established in multiple applications including wind turbines [5]. To add fault–tolerance to the common LPV and fuzzy controller formulation, different approaches can be exploited. For example, the AFTC scheme can use the parameters of both the LPV and fuzzy structures estimated by the FDD module for scheduling the controllers [19, 15]. On the other hand, different approaches can be used to obtain fault–tolerance in the PFTC methods. For this purpose, the design methods described in [5, 20] can be modified to cope with parametric uncertainties, as addressed *e.g.* in [21]. Alternatively, other methods could have been used such as [22], which preserves the nominal performance. Generally, these approaches rely on solving some optimisation problems where a controller is calculated subject to maximising the disturbance attenuation.

6. Conclusion

This paper revised the most important modelling and control issues on wind turbines from a systems and control engineering point of view. A walk around the wind turbine control loops discussed the goals of the most common solutions and overviews the typical actuation and sensing available on commercial turbines. The work intended to provide also an updated and broader perspective by covering not only the modelling and control of individual wind turbines, but also outlining a number of areas for further research, and anticipating new issues that can open up new paradigms for advanced control approaches. In summary, wind energy is a fast growing industry, and this growth has led to a large demand for better modelling and control of wind turbines. Uncertainty, disturbance and other deviations from normal working conditions of the wind turbines make the control challenging, thus motivating the need for advanced modelling and a number of so–called sustainable control approaches that should be explored to reduce the cost of wind energy. By enabling this clean renewable energy source to provide and reliably meet the world's electricity needs, the tremendous challenge of solving the world's energy requirements in the future will be enhanced. The wind resource available worldwide is large, and much of the world's future electrical energy needs can be provided by wind energy alone if the technological barriers are overcome. The application of sustainable controls for wind energy systems is still in its infancy, and there are many fundamental and applied issues that can be addressed by the systems and control community to significantly improve the efficiency, operation, and lifetimes of wind turbines.

References

[1] Johnson K E and Fleming P A 2011 *Mechatronics* **21** 728–736 DOI: 10.1016/j.mechatronics.2010.11.010
[2] Global Wind Energy Council 2014 Wind Energy Statistics 2013 Report
[3] Pao L Y and Johnson K E 2009 *Proceedings of the American Control Conference, 2009 – ACC'09*

(St. Louis, MO, USA: IEEE) pp 2076–2089 ISSN: 0743–1619. ISBN: 978–1–4244–4523–3. DOI: 10.1109/ACC.2009.5160195

[4] Laks J H, Pao L Y and Wright A D 2009 *Proceedings of the American Control Conference, 2009 – ACC'09* (St. Louis, MO, USA: IEEE) pp 2096–2103 ISSN: 0743–1619. ISBN: 978–1–4244–4523–3. DOI: 10.1109/ACC.2009.5160590

[5] Bianchi F D, Battista H D and Mantz R J 2007 *Wind Turbine Control Systems: Principles, Modelling and Gain Scheduling Design* 1st ed Advances in Industrial Control (Springer) ISBN: 1–84628–492–9

[6] Odgaard P F, Stoustrup J and Kinnaert M 2013 *IEEE Transactions on Control Systems Technology* **21** 1168–1182 ISSN: 1063–6536. DOI: 10.1109/TCST.2013.2259235

[7] Chen J and Patton R J 1999 *Robust Model–Based Fault Diagnosis for Dynamic Systems* (Boston, MA, USA: Kluwer Academic Publishers)

[8] Ding S X 2008 *Model–based Fault Diagnosis Techniques: Design Schemes, Algorithms, and Tools* 1st ed (Berlin Heidelberg: Springer) ISBN: 978–3540763031

[9] Isermann R 2005 *Fault–Diagnosis Systems: An Introduction from Fault Detection to Fault Tolerance* 1st ed (Weinheim, Germany: Springer–Verlag) ISBN: 3540241124

[10] Jonkman J M and Buhl Jr M L 2005 FAST User's Guide Tech. Rep. NREL/EL–500–38230 National Renewable Energy Laboratory Golden, CO, USA

[11] Georg S, Schulte H and Aschemann H 2012 *Proceedings of the IEEE International Conference on Fuzzy Systems* (Brisbane, Australia: IEEE) pp 1737–1744 ISSN: 1098–7584. ISBN: 978–1–4673–1507–4. DOI: 10.1109/FUZZ–IEEE.2012.6251302

[12] Simani S and Castaldi P 2014 *International Journal of Robust and Nonlinear Control* **24** 1283–1303 John Wiley. DOI: 10.1002/rnc.2993

[13] Odgaard P F and Johnson K 2013 *Proc. of the 2013 American Control Conference – ACC* (Washington DC, USA: IEEE Control Systems Society & American Automatic Control Council) pp 4447–4452 ISSN: 0743–1619. ISBN: 978–1–4799–0177–7

[14] Johnson K E, Pao L Y, Balas M J and Fingersh L J 2006 *IEEE Control Systems Magazine* **26** 70–81 DOI: 10.1109/MCS.2006.1636311

[15] Simani S and Castaldi P 2013 *Control Engineering Practice* **21** 1678–1693 special Issue Invited Paper. ISSN: 0967–0661. PII: S0967–0661(13)00155–X. DOI: http://dx.doi.org/10.1016/j.conengprac.2013.08.009

[16] Pao L Y and Johnson K E 2011 *IEEE Control Systems Magazine* **31** 44–62

[17] Mahmoud M, Jiang J and Zhang Y 2003 *Active Fault Tolerant Control Systems: Stochastic Analysis and Synthesis* Lecture Notes in Control and Information Sciences (Berlin, Germany: Springer–Verlag) ISBN: 3540003185

[18] Odgaard P F and Stoustrup J 2013 *Proceedings of the IEEE Multiconference on Systems and Control – MSC2013* (Hyderabad, India) pp 1–6

[19] Sami M and Patton R J 2012 *Proceedings of the 8th IFAC Symposium on Fault Detection, Supervision and Safety of Technical Processes – SAFEPROCESS 2012* vol 8 ed Verde C, Astorga Zaragoza C M and Molina A (National Autonomous University of Mexico, Mexico City, Mexico) pp 349–354 DOI: 10.3182/20120829–3–MX–2028.00131

[20] Galdi V, Piccolo A and Siano P 2008 *IEEE Transactions on Energy Conversion* **23**

[21] Puig V 2010 *International Journal of Applied Mathematics and Computer Science* **20** 619–635 DOI: 10.2478/v10006–010–0046–y

[22] Niemann H and Stoustrup J 2005 *International Journal of Control* **78** 1091–1110